radiative neon molecule.

ACKNOWLEDGMENTS

The author is grateful to G. S. Hurst, G. Payne, N. Thonnard, and R. E. Knight for interesting and helpful discussions. Particular thanks are due to G. S. Hurst and G. Payne for reading the manuscript. Numerical calculations were carried out using facilities of the University of Kentucky Computing Center.

[1]N. Thonnard and G. S. Hurst, Phys. Rev. A **5**, 1110 (1972).
[2]D. M. Bartell, Ph.D. thesis (University of Kentucky, 1972) (unpublished).
[3]J. E. Parks, Ph.D. thesis (University of Kentucky, 1970) (unpublished).
[4]T. E. Stewart, G. S. Hurst, T. E. Bortner, J. E. Parks, F. W. Martin, and H. L. Weidner, J. Opt. Soc. Am. **60**, 1290 (1970).
[5]T. E. Stewart, Ph.D. thesis (University of Kentucky, 1970) (unpublished).
[6]G. S. Hurst, T. E. Stewart, and J. E. Parks, Phys. Rev. A **2**, 1717 (1970).
[7]H. L. Weidner, University of Kentucky (unpublished).
[8]N. Thonnard, Ph.D. thesis (University of Kentucky, 1971) (unpublished).
[9]The energy levels are taken from C. E. Moore, *Atomic Energy Levels*, Natl. Bur. Stds. Circ. No. 467 (U. S. GPO, Washington, D.C., 1949), Vol. 1, p. 77.
[10]G. H. Shortley, Phys. Rev. **47**, 295 (1935).
[11]Y. Tanaka, A. S. Jursa, and F. J. LeBlanc, J. Opt. Soc. Am. **48**, 304 (1958).
[12]G. S. Hurst, T. E. Bortner, and T. D. Strickler, Phys. Rev. **178**, 4 (1969).
[13]T. Holstein, Phys. Rev. **72**, 1212 (1947).
[14]T. Holstein, Phys. Rev. **83**, 1159 (1951).
[15]G. M. Lawrence and H. S. Liszt, Phys. Rev. **178**, 122 (1969).
[16]A. V. Phelps, Phys. Rev. **114**, 1011 (1959).
[17]E. E. Wisniewski, J. T. Verdeyen, and B. E. Cherrington, Bull. Am. Phys. Soc. **16**, 206 (1971).

PHYSICAL REVIEW A VOLUME 8, NUMBER 2 AUGUST 1973

Formulation of the Binary-Encounter Approximation in Configuration Space and Its Application to Ionization by Light Ions*

J. S. Hansen
Cyclotron Institute, Texas A&M University, College Station, Texas 77843
(Received 20 February 1973)

The binary-encounter approximation (BEA) is transformed from momentum space to configuration space. In this frame the impact-parameter representation allows one to calculate a variety of quantities pertinent to the general problem of ionization. Among these are cross sections for proton ionization of hydrogen and helium; in the latter case, cross sections for ejection of both electrons are also given. A number of tables and formulas are given, enabling one to correct the simple hydrogenlike-model predictions of the BEA for effects which arise in multielectron atoms. Multiple-ionization probabilities ($K + L$ shell) are calculated and compared to experimental results and to the predictions of the semiclassical approximation.

I. INTRODUCTION

A vast amount of literature over the past several years has been devoted to experimental and theoretical inquiries into the effects which arise when a charged particle passes through an atomic charge cloud. With increased enthusiasm and ingenuity, researchers have obtained experimental results which refute many of the simplest predictions of the prevailing theories. Although many of these theoretical failures may arise because of the often concomitant alteration of the atom and hence its resemblance with the simple model by which it may be theoretically described, these same failures have created an environment stimulating to the theoretical reinvestigation of some of the details of charged-particle atomic collisions.

The present paper is presented with two distinct objectives in mind. The first goal is one of formulating in configuration space a model of the interaction of two charged particles, a bound electron and a particle of fixed trajectory with respect to the nucleus. The model evolves from a transformation of the widely used binary-encounter approximation (BEA) from momentum space into configuration space and then through a reexpression in the impact-parameter representation. The latter representation enables one to view the interaction process in terms of *probabilities* from which the cross sections can be obtained.

This representation (impact parameter) shows in a natural way that possible violations of probability conservation can lead to erroneous conclusions in the heretofore applied BEA. As a consequence, we shall distinguish between two distinct BEA theories which shall be called in the present text the "unconstrained BEA" and the "constrained BEA." The predictions of the former of these two theories yields identical results in either its momentum-space or configuration-space representation. The predictions of the latter theory lead to cross sections whose magnitude is less than the conventional (unconstrained) BEA.

The second goal is the task of modifying the BEA such that it can more readily account for discrepancies which arise because of differences between the real system of complex atom and particle and the theoretical system of hydrogenlike atom and particle. This task, the author realizes, can be only partially fulfilled with the simple formulas and tables as presented here, but these may be useful nevertheless in the interpretation of certain experimental anomalies which may arise in such collisions.

The present paper deals solely with the process of ionization by light ions and, as a consequence, ignores much of the work concerning atomic excitation and ionization by electrons or by heavy ions.

II. BACKGROUND

A classical theory of ionization was first developed by J. J. Thomson[1] in his effort to estimate the energy loss of charged particles in passing through matter. Being interested primarily in the interactions of fast incident particles and relatively slow, bound electrons he assumed that the velocity of all bound electrons was zero.

The BEA as formulated by Thomson gives only a qualitative description of the ionization process and hence, was for the most part ignored until Gryziński[2-4] presented his comprehensive papers on the classical theory of ionization. In these papers Gryziński derived expressions describing the interaction of two charged particles in free space, in which the incident particle, with velocity v_1, transfers part of its energy to the field particle with velocity v_2. Summation over those interactions giving rise to energy exchanges exceeding a certain value ΔE yields a quantity $\sigma_{\Delta E}(v_1, v_2)$ useful in the calculation of ionization cross sections. Gryziński further developed a prescription for the velocity distribution of the field particles (bound electrons), until then assumed to be a δ function at zero velocity. The Gryziński theory was very successful when judged upon a basis of relative simplicity, versatility, and accuracy; consequently, it stimulated the interest of others in the field.

Gerjuoy[5] and Vriens[6] independently rederived the free-particle cross section (FPC) for particles of arbitrary mass, charge, and velocity and showed that failure to explicitly average the cross section with respect to directional distribution of field particles, as in the Gryziński theory, can lead to significant error. The expressions derived by Gerjuoy and Vriens give the exact classical free-particle cross sections for an assumed isotropic distribution of field-particle velocity vectors. Vriens has further shown[6] that this classical result for protons coincides exactly with the quantal result (i.e., interference terms arising in electron-electron collisions are negligible for proton-electron collisions).

The velocity distribution of the bound electrons, as prescribed by Gryziński, was for the most part derived semiempirically. A number of other authors[6-8] have presented results for the BEA estimates of the ionization cross section of atomic hydrogen by protons using a velocity distribution appropriate to the $1s$ state in atomic hydrogen. Their results for the ionization cross section $\bar{\sigma}_U(v_1)$ followed from averaging the correct[5,6] $\sigma_U(v_1, v_2)$ over this normalized velocity distribution. The subscript U indicates that the above-mentioned summation was conducted for all energy exchanges exceeding the binding energy U. Particularly noteworthy was an analytical derivation of $\bar{\sigma}_U(v_1)$ given by Vriens[6] who amongst others has also related the BEA to quantal theories.[9] Quite recently, the BEA has been applied to a variety of problems which include ionization of complex atoms by light ions. Garcia[8,10,11] and his coworkers have shown in a series of papers that the classical BEA for incident-particle velocities less than the mean velocity of the bound electron is comparable in accuracy to the predictions of the plane-wave Born approximation.[10]

In Ref. 12, an excellent review of the BEA has been given by Vriens. A comprehensive investigation of the underlying principles of this theory is undertaken and numerous comparisons of its predictions with the predictions of other theories and experimental results are made. Less detailed, yet complementary, discussions of the BEA are also to be found in Refs. 13 and 14.

III. BEA IN MOMENTUM SPACE

In the present section a general formulation for the BEA is given. This formulation indicated that the velocity distribution of the bound electron evolves directly from the (square of the) momentum-space wave function of the bound electron. Others authors[15,16] over the past several years

have employed a similar formulation, and in order to distinguish these results from the results of the classical BEA have referred to them as having been derived from the "quantal BEA."

The more commonly used "classical BEA" is seen to be derived from two approximations: (i) The velocity distribution for an electron in any subshell (n, l) is described by the $1s$ distribution and (ii) within the hydrogenlike wave function for the bound electron, the effective or screened charge divided by the principle quantum number n is replaced by the square root of the binding energy in rydberg units, i.e., $Z_{\rm eff}/n \to (U/R)^{1/2}$.

For ionization of the $1s$ state of hydrogen the classical BEA and general BEA predict identical results since $Z_{\rm eff}/n = (U/R)^{1/2} = 1$. For other electrons in other atoms, and particularly for electrons in subshells other than the $1s$, it is shown that the classical and general BEA lead to different predicted cross sections. Owing to a direct relationship between the average momentum distribution of any total shell n and the momentum distribution for the $1s$ shell, the classical BEA and the general BEA should lead to very nearly identical results for the total n shell cross sections.

The primary assumption within the theoretical framework of the BEA is that the bound electrons (field particles) can be treated as free insofar as their interaction with the incident projectile is concerned. As a consequence of this assumption the nucleus and other atomic electrons only play a passive role in aiding to determine the ionization potential and velocity distribution of the electron involved in the Coulombic collision with the incident charged particle. This binary, or two-particle, approximation to the ionization process, and additionally ignoring the consequence of any competitive processes which might occur for electrons receiving an energy exceeding their ionization potential, allows us to proceed within these approximations to a general formulation for the ionization process.

Given the free-particle cross section[17] $\hat{\sigma}_U(v_1, v_2)$ for each arbitrary field-particle velocity v_2, an average $\langle \hat{\sigma}_U(v_1, v_2) \rangle$ can be found contingent upon an accurate prescription for the probability of finding a bound electron between v_2 and $v_2 + dv_2$. The general or quantal BEA ionization cross section for an atomic shell containing N electrons can thus be formulated as[15,16]

$$\begin{aligned}\sigma_U(v_1) &= \sum_N \langle \hat{\sigma}_U(v_1, v_2) \rangle \\ &= \sum_N \int_0^\infty \hat{\sigma}_U(v_1, v_2) \rho_{nl}(v_2) 4\pi v_2^2 dv_2 \\ &= \sum_N \int_0^\infty f_{nl}(v_2) \hat{\sigma}_U(v_1, v_2) dv_2 , \end{aligned} \tag{3.1}$$

where $\rho_{nl}(v) = \phi_{nl}^*(v)\, \phi_{nl}(v)$ and $\phi_{nl}(v)$ is the solution to the Schrödinger equation in momentum (velocity) space.[18]

Perhaps of even greater significance than the derivation of $\phi_{nl}(v)$ from Schrödinger's equation in momentum space is the fact that these same $\phi_{nl}(v)$ are directly related to the $\psi_{nl}(r)$ in configuration space through the Fourier transformation.[18,19] Consequently, we conclude that the most accurate $f_{nl}(v)$ must directly follow from our best (Hartree-Fock) description of the $\psi_{nl}(r)$. This has been recognized earlier,[20,21] and in efforts to test the predictions of the BEA for simple systems, $f_{nl}(v)$ has been derived directly from numerical momentum-space Hartree-Fock wave functions following a Fourier transformation from configuration space.[15,20,21]

The prescription most widely used[8,10,11] for $f_{nl}(v)$ is

$$f_{nl}(v) = \frac{32}{\pi} U^{5/2} \frac{v^2}{(U + v^2)^4} , \tag{3.2a}$$

where U is the binding energy in rydbergs (1 Ry $= 13.6$ eV) and v is in units of αc ($1\alpha c = 7.3\times10^{-3} \times 2.998\times10^{10}$ cm/sec). The inverse Fourier transformation leads us to

$$\begin{aligned}\tilde{f}_{nl}(r) &= 4r^2 U^{3/2}\, e^{-2rU^{1/2}} \\ &= 4\pi r^2 \tilde{\rho}_{nl}(r) = 4\pi r^2 \phi_{nl}^*(r)\, \psi_{nl}(r), \end{aligned} \tag{3.2b}$$

and we find that

$$\psi_{nl}(r) = U^{3/4} e^{-rU^{1/2}}/\pi^{1/2}, \tag{3.2c}$$

where r is the electron distance from the nucleus in units of Bohr radii ($a_0 = 5.29\times10^{-9}$ cm). This for the $1s$ state of hydrogen gives

$$\psi_{1s} = Z_{\rm eff}^{3/2} e^{-Z_{\rm eff} r}/\pi^{1/2}, \tag{3.3}$$

with $Z_{\rm eff} = 1 = U^{1/2}$. For an electron in the $1s$ state of a multielectron atom, a more accurate wave function ψ_{1s} is probably found by replacing $Z_{\rm eff}$ in Eq. (3.3) by $Z - 0.3$,[18] rather than by $U^{1/2}$, as in Eq. (3.2c). The use of the approximation $Z_{\rm eff} = U^{1/2}$ does lead to a very convenient scaling law, namely,[10]

$$\sigma_{\rm ion}(E_1', U_b) = (U_a^2/U_b^2)\, \sigma_{\rm ion}(E_1, U_a), \tag{3.4}$$

where $E_1' = (U_b/U_a) E_1$. Here E_1 and E_1' are the energies of particles incident upon electrons having binding energies U_a and U_b, respectively. These simple scaling laws have facilitated comparisons of experimental and theoretical cross sections for atoms with different binding energies. Equation (3.2a) is also directly derivable from a classical microcanonical ensemble of particles, and in this context we might consider predictions based upon this premise as being derived from the "classical BEA."

For subshells other than the $1s$, use of the classical momentum distribution f_{1s} rather than the momentum distribution f_{nl} can lead to significant error. Because each of the proper momenta distributions f_{nl} gives rise to identical scaling properties as given in Eq. (3.4) (provided we replace Z_{eff}^2/n^2 by U/Ry in their respective wave functions), we have tabulated these scaled cross sections for the L subshells (Table I). As an example we calculate the ionization cross section per $2p$ electron in Ti ($U = 500$ eV) for 250-keV incident α particles. We find

$$v_1^2/\bar{v}^2 = (E_1/M_1)(m/U) = \frac{250\ \text{keV}}{(4)(1836)(0.5\ \text{keV})^2} = 0.136.$$

The cross section corresponding to this value of $v_1^2/\bar{v}^2$ is therefore q^2/U^2 multiplied by the value found in the last column in the table yielding $\hat{\sigma} \simeq 9\times10^4$ b per electron. The classical BEA cross section is seen to be smaller by a ratio of approximately $4.7/5.5 = 0.85$.

In Fig. 1 we compare the momenta distributions for the $1s$, $2s$, and $2p$ states of (hydrogenlike) atoms having equivalent binding energies. Using the values from Table I, we can calculate the cross sections for ionization of the $2s$ and $2p$ subshells of Au by protons (Figs. 2 and 3) and directly compare them to the results of the classical BEA, the semiclassical approximation (SCA)[22] and the plane-wave Born approximation (PWBA).[23] Direct comparison of the classical BEA and the more appropriate descriptions $\sigma[f_{2s}(v)]$ and $\sigma[f_{2p}(v)]$ indicate that the total cross sections are for the most part insensitive to the details of the momenta distributions (Fig. 1).

Of further consequence is a rule derived by Fock[24] which shows that for fully occupied and degenerate substates (n, l), the *average* momentum distribution of the total shell (n) is identical with $f_{1s}(v)$. That is to say

$$\rho_{1s}(v) = \tfrac{1}{8}[2\rho_{2s}(v) + 6\rho_{2p}(v)], \tag{3.5}$$

which can easily be substantiated by referring to Fig. 1. Therefore, provided Fock's conditions are not too strongly violated, comparison of *total* cross sections for a particular shell (n) will lead to similar results regardless of whether one uses the exact descriptions of $f_{nl}(v)$ for each subshell or averages the FPC over the classical $f_{1s}(v)$ distribution with an assumed weighted mean binding energy. Comparisons of this sort have not been carried out but the results of the classical prediction for the total L-shell cross section of Au have been made with the PWBA and with experimental results, and all have been found[23] to be in very close agreement. The predictions[22] of the SCA (Figs. 2 and 3) are widely divergent from any of the other theories suggesting perhaps an error in the numerical calculations for the $2s$ and $2p$ states.[25,26]

TABLE I. BEA cross sections per electron. $(\hat{\sigma}U^2/z^2)$ [b (keV)^2].

$\left(\frac{v_1}{\bar{v}}\right)^2 = \frac{mE_1}{M_1U}$	$1s$	$2s$	$2p$
2.00×10^{-3}	1.23×10^{-3}	6.0×10^{-3}	9.1×10^{-5}
2.70×10^{-3}	1.23×10^{-2}	4.73×10^{-2}	1.42×10^{-3}
3.65×10^{-3}	4.36×10^{-2}	1.54×10^{-1}	5.8×10^{-3}
4.92×10^{-3}	1.40×10^{-1}	4.93×10^{-1}	2.62×10^{-2}
6.64×10^{-3}	4.42×10^{-1}	1.45×10^{0}	1.09×10^{-1}
8.97×10^{-3}	1.30×10^{0}	3.96×10^{0}	4.15×10^{-1}
1.21×10^{-2}	3.71×10^{0}	1.02×10^{1}	1.53×10^{0}
1.63×10^{-2}	1.04×10^{1}	2.50×10^{1}	5.45×10^{0}
2.21×10^{-2}	2.82×10^{1}	5.70×10^{1}	1.86×10^{1}
2.98×10^{-2}	7.4×10^{1}	1.18×10^{2}	5.95×10^{1}
4.02×10^{-2}	1.88×10^{2}	2.19×10^{2}	1.77×10^{2}
5.43×10^{-2}	4.56×10^{2}	3.60×10^{2}	4.89×10^{2}
7.32×10^{-2}	1.06×10^{3}	5.5×10^{2}	1.23×10^{3}
9.89×10^{-2}	2.31×10^{3}	9.65×10^{2}	2.76×10^{3}
1.33×10^{-1}	4.67×10^{3}	2.32×10^{3}	5.5×10^{3}
1.80×10^{-1}	8.7×10^{3}	6.2×10^{3}	9.55×10^{3}
2.43×10^{-1}	1.48×10^{4}	1.45×10^{4}	1.49×10^{4}
3.28×10^{-1}	2.27×10^{4}	2.71×10^{4}	2.13×10^{4}
4.43×10^{-1}	3.15×10^{4}	4.05×10^{4}	2.85×10^{4}
5.98×10^{-1}	3.93×10^{4}	4.94×10^{4}	3.60×10^{4}
8.08×10^{-1}	4.43×10^{4}	5.10×10^{4}	4.22×10^{4}
1.09×10^{0}	4.51×10^{4}	4.38×10^{4}	4.53×10^{4}
1.47×10^{0}	4.31×10^{4}	3.91×10^{4}	4.44×10^{4}
1.99×10^{0}	3.81×10^{4}	3.25×10^{4}	4.00×10^{4}
2.68×10^{0}	3.20×10^{4}	2.68×10^{4}	3.37×10^{4}
3.62×10^{0}	2.57×10^{4}	2.20×10^{4}	2.70×10^{4}
4.88×10^{0}	2.02×10^{4}	1.78×10^{4}	2.09×10^{4}
6.59×10^{0}	1.55×10^{4}	1.42×10^{4}	1.59×10^{4}
8.90×10^{0}	1.18×10^{4}	1.10×10^{4}	1.20×10^{4}
1.2×10^{1}	8.8×10^{3}	8.4×10^{3}	9.0×10^{3}
1.62×10^{1}	6.6×10^{3}	6.4×10^{3}	6.6×10^{3}
2.95×10^{1}	3.66×10^{3}	3.62×10^{3}	3.68×10^{3}

IV. TRANSFORMATION OF BEA INTO CONFIGURATION SPACE

Gryziński has pointed out that the BEA may be described in configuration space by[4]

$$\sigma_U(v_1) = \sum_N \int_0^\infty \hat{\sigma}_U[v_1(r),\ v_2(r)]\,\tilde{\rho}(r)4\pi r^2\,dr. \tag{4.1}$$

The problem heretofore in using such a formulation has been that of developing a suitable and consistent relationship between the velocity of a bound electron and its distance from the nucleus. In order that such a transformation be successful one must satisfy two criteria: (a) The solution of Eq. (4.1) for $\sigma(v_1)$ must be identical to the solution of Eq. (3.1) and (b) the transformation must lead to physically plausible results for $v(r)$.

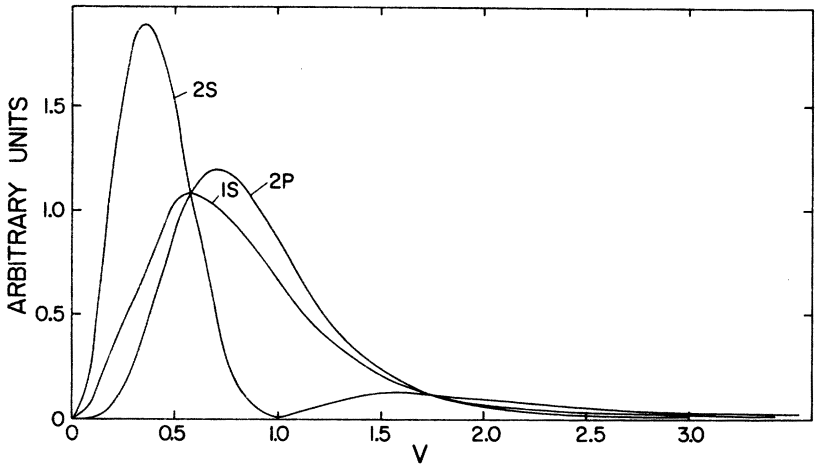

FIG. 1. Distribution functions, for the $1s$, $2s$, and $2p$ states, describing the relative probability of finding an electron with a velocity v. The distribution functions are normalized such that the total energy of the states are equivalent.

The first criterion is met by requiring for arbitrary velocity v_2 that the probability for finding the electron with a velocity between v_2 and v_2+dv_2 be identical in both momentum space and in configuration space. Innumerable solutions satisfying criterion (a) are available but we must select from these a solution that will also satisfy criterion (b), i.e., the magnitude of the velocity of an electron as a function of its distance from the nucleus must be physically plausible. In order to meet

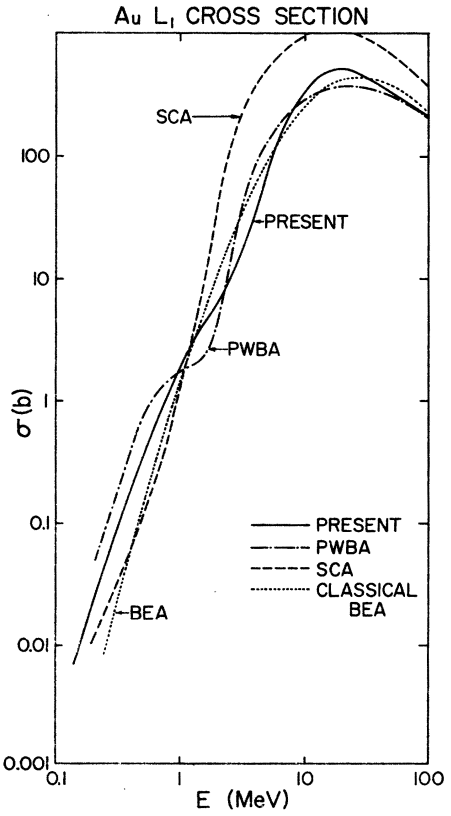

FIG. 2. Theoretical proton-ionization cross sections for the $2s(L_1)$ state of gold. The curve labeled BEA uses the classical $f_{1s}(v)$ distribution, whereas the present calculation uses the more appropriate $f_{2s}(v)$ distribution (see text). PWBA: Ref. 23; SCA: Ref. 22.

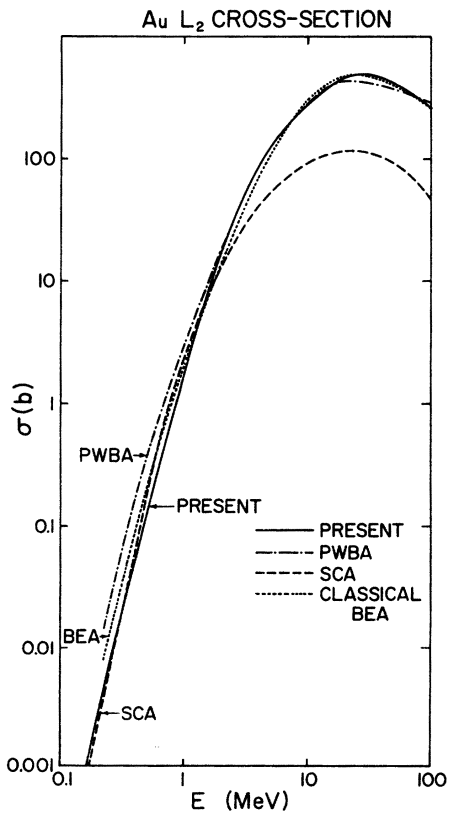

FIG. 3. Theoretical proton-ionization cross sections for the $2p_{1/2}(L_2)$ state of gold. The curve labeled BEA uses the classical $f_{1s}(v)$ distribution; present calculation uses the $f_{2p}(v)$ distribution. PWBA: Ref. 23; SCA: Ref. 22.

the second criterion, we may first observe that the probability distribution functions $\tilde{f}_{nl}(r)$ and $f_{nl}(v)$ permit[18] all finite and real values of distance and velocity in configuration and momentum space, respectively. Second, we observe that from both the Heisenberg uncertainty principle and the law of total-energy conservation it is predicted that as the radial distance becomes diminishingly small, the electron's velocity becomes unlimitingly large. Thus with the condition that criterion (a) be satisfied and further, that the velocity of the electron, v', increases to infinity as its distance from the nucleus, r', decreases to zero, we deduce the following relationship between v' and r':

$$\int_{v'}^{\infty} \rho_{nl}(v) 4\pi v^2 dv - \int_0^{r'} \tilde{\rho}_{nl}(r) 4\pi r^2 dr = 0, \qquad (4.2)$$

where the $\rho_{nl}(v)4\pi v^2 = f_{nl}(v)$ and $\tilde{\rho}_{nl}(r)4\pi r^2 = \tilde{f}_{nl}(r)$ have been defined in Sec. III.

The predicted magnitudes of the velocity for an electron in the $1s$, $2s$, or $2p$ shells of hydrogen are given in Figs. 4 and 5. In these figures, the $v(r)$ relationship from Eq. (4.2) is compared with a classical definition based solely upon the conservation of total energy. The present prescription differs from this classical definition primarily in the fact that in the so-called "nonclassical" domain,[27] where the classical description predicts negative kinetic energy (imaginary velocities), the present description predicts velocities both finite and real. Use of the classical definition in the case of subshells with angular momentum quantum number $l > 0$, e.g., $2p$ subshell, leads to a nonclassical region at small r as well as at large r. Consequently, using the purely classical definition leads to the implausible conclusion that

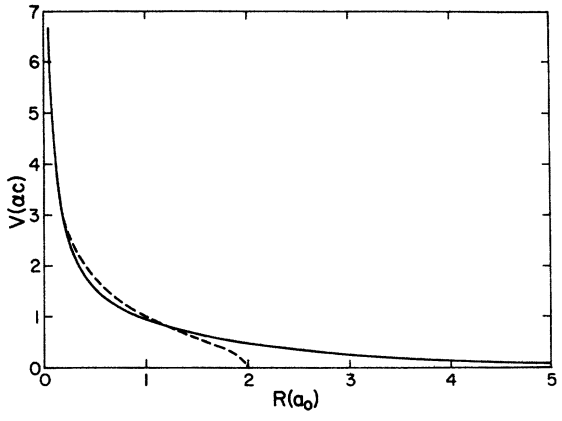

FIG. 4. Average velocity of an electron in the ground state of hydrogen as a function of its distance from the nucleus. Solid curve: estimate from Eq. (4.2); dashed curve: classical estimate from conservation of total energy. Velocities in the latter case become imaginary for $r/a_0 > 2$.

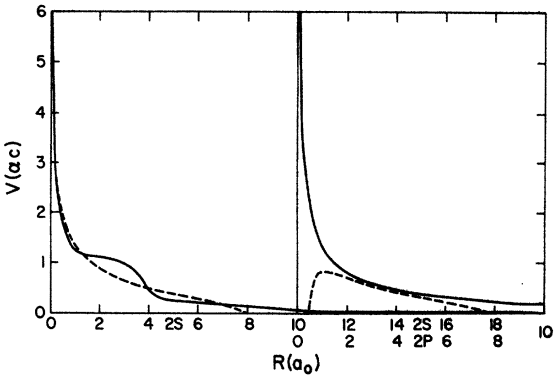

FIG. 5. Velocity of an electron as a function of its distance from the nucleus for the $2s$ and $2p$ states of hydrogen. Curves have the same significance as in Fig. 4.

although the probability of finding an electron at small or large r remains finite, our best estimate for its velocity nevertheless is undefined, i.e., the kinetic energy is negative. Owing to the admission by the probability distribution functions of all velocities and distances between zero and infinity, the present formulation overcomes these physically unacceptable solutions.

The use of screened hydrogenic wave functions in Eq. (4.2) gives the following relationship between the velocity of an electron in an atom of effective nuclear charge Z_{eff} and the velocity of an electron in hydrogen:

$$v_{Z_{\text{eff}}}(r) = Z_{\text{eff}} v_{\text{H}}(rZ_{\text{eff}}). \qquad (4.3)$$

As stated above, Eq. (4.1) [where $v(r)$ is found from Eqs. (4.2) and (4.3)] will predict identical results for $\sigma(v_1)$ as that found from the momentum-space formulation, Eq. (3.1). One must of course use a definition for $\tilde{\rho}_{nl}(r) = \psi^*_{nl}(r)\psi_{nl}(r)$ consistent[28] with the choice of Z_{eff} in Eq. (4.3) [see, for example, Eq. (3.3)].

Having the BEA in configuration space allows Eq. (4.1) to now be transformed from spherical to cylindrical coordinates, thus giving the impact-parameter representation[29]

$$\sigma(v_1) = \sum_N \int_0^{\infty} 2\pi b \hat{P}_{v_2(r)}(b, v_1)\, db. \qquad (4.4)$$

Here we explicitly indicate that although [provided criterion (a) is satisfied] $\sigma(v_1)$ is independent of the form of $v_2(r)$, the probability of ionization $P_{v_2(r)}(b, v_1)$ does depend upon the details of the description of $v_2(r)$. The total cross section for a particular shell in an atom is found by summing the cross section per electron over the number of electrons as in Eqs. (3.1) and (4.1).

In Fig. 6, a test of the validity of our relationship for $v(r)$ is provided through a comparison of the

present calculated total probability of ionization of the 1s shell of Se with the experimental results of Laegsgaard *et al.*[30] In this figure the probability of ionization per electron $[\hat{P}_{\nu_2(r)}(b,v_1)$, in Eq. (4.4)] has been multiplied by 2 to account for the two electrons occupying the 1s shell.

V. CONSTRAINED BEA ARISING FROM PROBABILITY CONSERVATION

To this point in the present paper, emphasis has been placed upon the equality of the predictions of the BEA whether calculated in momentum space or in configuration space. In this section we show that under certain circumstances that probability is not properly conserved in the conventional BEA, which until now has been formulated in momentum space exclusively. In configuration space, however, these probability violations become apparent and use of a properly unitarized form of the ionization probability leads to substantially different predictions in cases where the probability of ionization is of the order of unity. These predictions, based upon a unitarized probability, shall be called the predictions of the (probability) constrained BEA and in context the predictions of the conventional BEA shall then be referred to as the unconstrained BEA predictions.[31,32]

In order to facilitate notation, the preceding equation shall be rewritten as

$$\sigma = \int_0^\infty 2\pi b P(b)\, db, \tag{5.1}$$

where $P(b)$ is the total ionization probability for a particle traveling in the direction of increasing z with an impact parameter b. For a given incident-particle rate, $R(-\infty)$ at $Z=-\infty$, the probability of ionization may be defined as $P(b)=1-R(\infty)/R(-\infty)$, where $R(\infty)$ then represents the number of particles per unit time at $Z=\infty$ which have not been involved in ionization of one of the bound electrons. Defined in this manner, the ratio $R(\infty)/R(-\infty)$ may be found from solving the following differential equation:

$$dR(z) = \left(\frac{R(z)}{2\pi b\, db}\right)[\sigma(b^2+z^2)^{1/2}][2\pi b\, db\, dz\, \tilde{\rho}_N(b^2+z^2)^{1/2}]. \tag{5.2}$$

The number of ionizations which take place per unit time between z and $z+dz$ in a circular ring of inner and outer radius of b and $b+db$, respectively, and whose plane is normal to the z axis is given in Eq. (5.2) as the product of the particle flux, cross section per electron, and number of field particles in the volume $2\pi b\, db\, dz$. The field-particle density $\tilde{\rho}_N(b^2+z^2)^{1/2}$ for a shell containing N electrons may be approximated by the product of the number of electrons in the shell and

$$\tilde{\rho}(b^2+z^2)^{1/2} = \psi^*(r)\psi(r).$$

The probability of ionization, $P(b)$, derived from Eq. (5.2), is the constrained-BEA definition of the probability of ionization:

$$P(b) = 1 - \frac{R(+\infty)}{R(-\infty)} = 1 - \exp(-N\int_{-\infty}^{\infty} \tilde{\rho}(r)\sigma(r)dz)$$

constrained BEA. (5.3)

As the magnitude of the integral becomes small with respect to unity, Eq. (5.3) reduces to the following:

$$P(b) = N\int_{-\infty}^{\infty} \tilde{\rho}(r)\sigma(r)dz$$

unconstrained BEA. (5.4)

Using Eq. (5.1) and $P(b)$ as defined by Eq. (5.4) yields identical cross sections as found in the conventional or momentum-space BEA, whereas $P(b)$ as defined in Eq. (5.3) leads, in general, to cross sections smaller in magnitude than the conventional BEA.

The probability of ionization per electron, $\hat{P}(b)$, is related to the total ionization probability $P(b)$ by

$$P(b) = 1 - [1 - \hat{P}(b)]^N, \tag{5.5}$$

where $\hat{P}(b)$ is given by

$$\hat{P}(b) = 1 - \exp[-\int_{-\infty}^{\infty} \tilde{\rho}(r)\sigma(r)dz]. \tag{5.6}$$

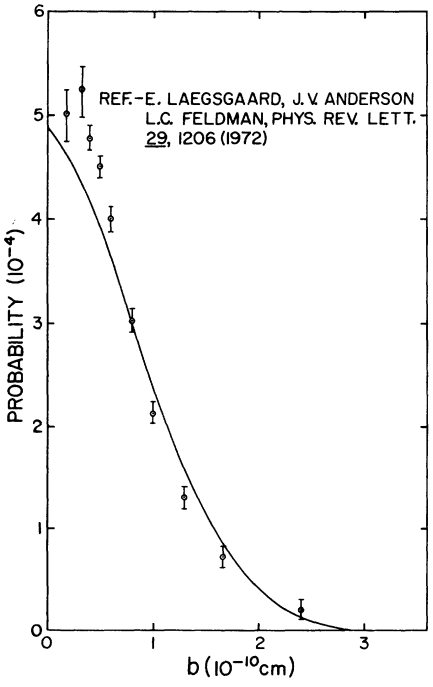

FIG. 6. Probability of proton ionization of the 1s state (K shell) of selenium. Solid curve: present theoretical results. Experimental values taken from Ref. 30.

Equation (5.6) when substituted into the preceding equation, (5.5), therefore produces the constrained-BEA definition of $P(b)$.

In certain cases it is convenient to define the total cross section as

$$\sigma = N\int_0^\infty 2\pi b\,db\,\hat{P}(b), \tag{5.7}$$

with $\hat{P}(b)$ given by the preceding expression. This approximation will be sufficiently accurate provided $\hat{P}^2(b) \ll 2\hat{P}(b)/(N-1)$, as can be verified by expanding the right-hand side of Eq. (5.5).

Differences in the magnitude of the constrained- and unconstrained-BEA cross sections will be negligible provided that Eq. (5.4) is a close approximation of Eq. (5.3). In the following section we shall compare the proton-ionization probabilities and cross sections for hydrogen calculated from the constrained- and unconstrained-BEA theories. We shall estimate here the approximate binding-energy and projectile-charge (q) dependence of the integral given in these equations and show that provided $U/q^2N \gg 1$ Ry, that differences between the constrained- and unconstrained-BEA cross sections will be negligible.

Let us define the probability of ionization by a fixed-velocity particle of charge q traversing some impact parameter b in an atom containing N electrons, each with binding energy U, as

$$P_U(b) = N\int_{-\infty}^{\infty} \sigma_U[v_2(r)]\,\tilde{\rho}_U(r)\,dz, \quad r = (b^2+z^2)^{1/2}.$$

Accepting the classical assumption (Sec. III) that we may replace Z_{eff}/n by $(U/\text{Ry})^{1/2}$, and further that the $1s$ velocity distribution is sufficiently accurate in its description of the distribution of an electron in any shell provided the energy per nucleon of the projectile of charge q is U times greater than that of the proton interacting with hydrogen, then the free-particle cross section for ionization of an electron with binding energy U by a particle of charge q is related to the free-particle proton-ionization cross section of hydrogen by[11]

$$\sigma_U(v_2) = \frac{q^2\sigma_{\text{H}}(v_2/U^{1/2})}{U^2}.$$

The charge density in hydrogenlike atoms is normalized[18] such that within the above assumptions

$$\tilde{\rho}_U(r) = U^{3/2}\,\tilde{\rho}_H(rU^{1/2}).$$

By using Eq. (4.3), we therefore find

$$P_U(b) = N\int_{-\infty}^{\infty} \frac{q^2\sigma_H[v_2(rU^{1/2})]}{U}\,\tilde{\rho}_H(rU^{1/2})\,U^{1/2}\,dz$$

$$= \frac{q^2NP_H(bU^{1/2})}{U/\text{Ry}}. \tag{5.8}$$

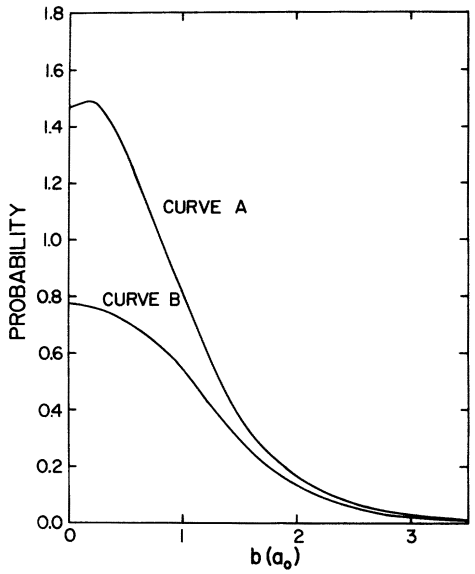

FIG. 7. Probability of ionization of the $1s$ state of hydrogen by 25-keV incident protons. Curve A results from a direct transformation of the BEA from momentum space and is calculated using Eq. (5.4). Curve B is the constrained BEA ionization probability calculated from Eq. (5.3).

Thus in general Eq. (5.4) will be a close approximation to Eq. (5.3) provided $U/q^2N \gg 1$ Ry.

VI. APPLICATION OF CONFIGURATION-SPACE BEA

A. Ionization of Hydrogen and Helium by Protons

In Fig. 7 are shown the constrained- and unconstrained-BEA proton-ionization probabilities for ground-state hydrogen as a function of impact parameter. Curve A has been calculated from Eq. (5.4) and when integrated according to Eq. (5.1) yields the exact results as given by the conventional BEA. Curve B has been computed from Eq. (5.3) and when this equation is integrated according to Eq. (5.1), cross sections smaller in magnitude than the conventional BEA result. In Fig. 8, proton-ionization cross sections resulting from these two approaches are compared with the available experimental results. The experimental data at low energies are in better agreement with the constrained-BEA calculation, whereas the high-energy results are in better agreement with the unconstrained-BEA calculation. The fact that the two sets of experimental data do not appear consistent will hopefully provide incentive for further measurements.

Envisioning the ionization process as occurring event by event, we can express Eq. (5.1) in the following manner:

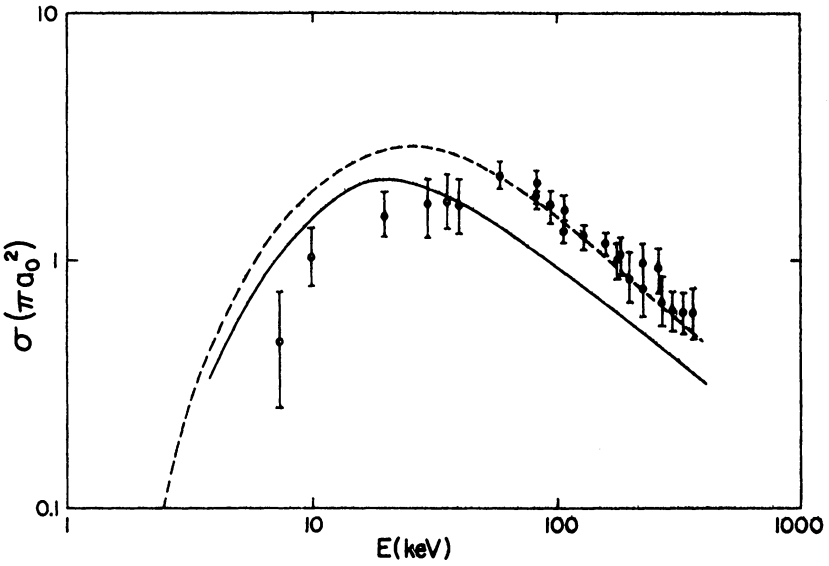

FIG. 8. Comparison of the measured ionization cross section of hydrogen with the constrained and unconstrained BEA. Solid curve: constrained BEA; dashed curve: unconstrained BEA. Experimental values: Open circles, Ref. 33; solid circles, Ref. 34.

$$\sigma = \int_0^\infty 2\pi b\{\hat{P}_U(b)[1-\hat{P}_{U'}(b)] + [1-\hat{P}_U(b)]\hat{P}_U(b) + \hat{P}_U(b)\hat{P}_{U'}(b)\}\,db \tag{6.1}$$

$$= \sigma_1 + \sigma_2 . \tag{6.2}$$

The first term in braces represents the probability of ionizing the first electron in helium having a binding energy $U = 24.58$ eV $= 1.807$ Ry and not removing the second electron with binding $U' = 54.4$ eV $= 4$ Ry. The second term in braces represents the probability of not ejecting the first electron but ejecting the second electron. The final term represents the probability of removing both electrons, the first with binding energy U and the latter with binding energy U'. The first two processes lead to ejection of exactly one electron and the resulting partial cross section is designated as σ_1, whereas the latter process leading to ejection of both electrons is designated as σ_2. The sum of the three terms in braces is the total probability of ionization and is shown in Fig. 9 as a function of impact parameter for 100-keV protons. The probability of double ejection, given by the latter term in Eq. (6.1), is also shown in Fig. 9 and at small impact parameters is seen to occur during approximately 20% of the ionizations. The third curve in this figure is the total ionization probability as found using Eq. (5.4). Again as in the case of proton ionization of hydrogen, the predicted ionization probabilities exceed unity over a considerable range of impact parameters.

In general, these violations of unitarity will be somewhat more severe in the proton ionization of helium than in proton ionization of hydrogen. This is predicted by Eq. (5.8) and results from an inherent approximation in the unconstrained-BEA calculation that the total probability of ionization, $P(b)$, in helium is related to the ionization probability per electron, $\hat{P}(b)$, by $P(b) = 2\hat{P}(b)$. Use of such a definition in lieu of the unitarized definition, i.e., $P(b) = 2\hat{P}(b) - \hat{P}^2(b)$, leads to violations of unitarity for the individual $\hat{P}(b)$ exceeding 0.5 as opposed to ionization of hydrogen where violations occur only for $\hat{P}(b)$ exceeding unity.

In many experimental measurements one often is required to determine the ionization cross section from a measurement of the number of electrons ejected rather than from a measurement of

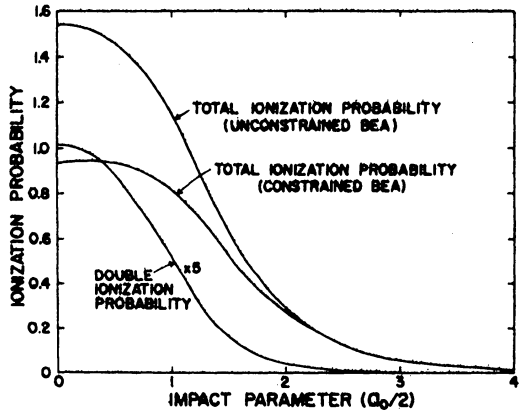

FIG. 9. Probabilities of ionization as a function of impact parameter for 100-keV protons incident upon helium. The lower curve which represents the probability of ejecting both electrons from helium has been multiplied by a factor of 5. The abscissa is in units of $\frac{1}{2}a_0 = 2.65 \times 10^{-9}$ cm.

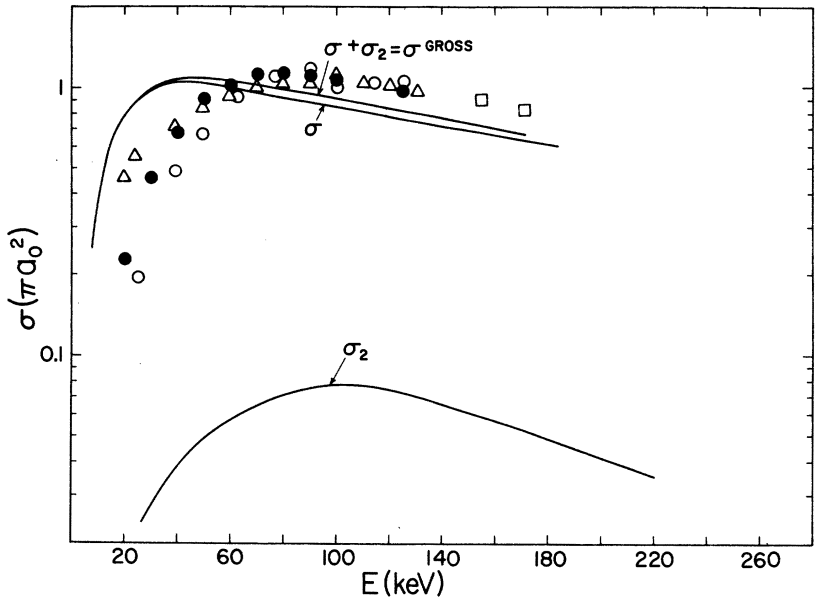

FIG. 10. Ionization of helium by protons. Lower curve: cross section for ejection of both electrons. Curve labeled σ designates the total calculated cross section. Upper curve is the gross cross section (see text). Experimental values: solid circles, Ref. 36; squares, Ref. 37; triangles, Ref. 38; open circles, Ref. 39.

the number of ionizations which occur, without regard for the number of electrons ejected. The latter of these two measurements is compatible with Eq. (6.1), the conventional definition of the ionization cross section. The former of these two measurements has been called[35] the gross ionization cross section and in general exceeds the conventional ionization cross section σ. The gross ionization cross section for a two-electron system such as helium is given by

$$\sigma^{\text{gross}} = \sigma_1 + 2\sigma_2 = \sigma + \sigma_2 . \tag{6.3}$$

In Fig. 10, the double-ionization cross section σ_2, ionization cross section σ, and gross cross section σ^{gross}, are presented for the proton-atomic-helium system. The latter two cross sections are compared with the available experimental results. It is difficult to determine which of the above-mentioned cross sections (σ or σ^{gross}) were measured in each experiment, but discrepancies between sets of measurements may arise partially from the effects of simultaneous ejection of both electrons which in the one case may have been accounted for but not in the other case.

The constrained-BEA proton-ionization cross sections of helium are compared to the predictions of the plane-wave Born approximation and the unconstrained BEA in Fig. 11. The constrained-BEA and the PWBA calculations are in reasonable agreement with one another at all energies although at high energies the PWBA calculations in general lie closer to the experimental results (compare with Fig. 10). On the other hand, in the region around 60 keV, where the experimental results and the PWBA and constrained-BEA calculations are all in good agreement, the magnitude of the unconstrained-BEA cross sections are approximately 70% greater. A gradual convergence of the constrained- and unconstrained-BEA cross sections will occur at very low and very high incident-particle energies as the probability of ionization becomes significantly less than unity. At very high energies the BEA calculations will decrease more rapidly with energy than the PWBA calculations owing to a neglect on the part of the

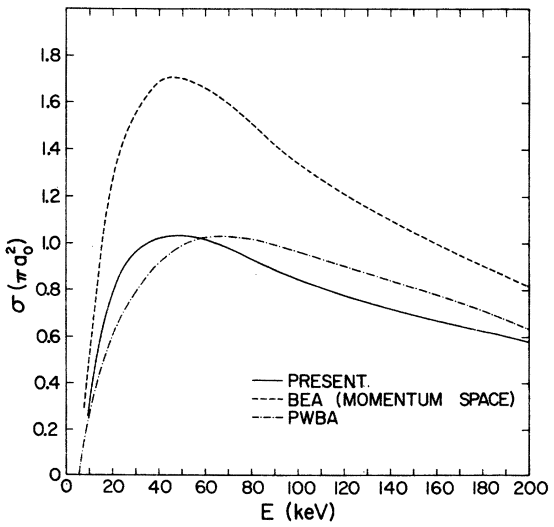

FIG. 11. Comparison of theoretical total ionization cross sections of helium by protons. Upper dashed curve: conventional BEA; solid curve: present constrained BEA; lower broken curve: PWBA calculation, Ref. 40.

BEA theory to account properly for interactions involving small momentum transfers.[9,35] The present calculations were carried out using an effective Z [Eqs. (6.1) and (6.2)] for the $1s$ shell of 1.7 in order to approximate the proper momentum distribution. This choice was made in the case of helium since large relative differences between the rule

$$Z_{\text{eff}} \simeq \left(\frac{U}{\text{Ry}}\right)^{1/2} = \left(\frac{24.58\ \text{eV}}{13.6\ \text{eV}}\right)^{1/2} = 1.3$$

and $Z_{\text{eff}} = 1.7$ occur. Vriens[21] has shown for the unconstrained BEA that cross sections calculated using the latter rule are in far better agreement with the results found in using two- and three-term Hartree-Fock wave functions than are the results using the former rule $Z_{\text{eff}} = 1.3$. Use of this "faster" momentum distribution has the effect, in both the constrained and unconstrained BEA, of increasing the calculated energy at which the cross section reaches its maximum, giving better agreement with the apparent experimental energy. The magnitude of the cross section at its maximum value is also found to diminish slightly in the present case with the use of this faster momentum distribution. Catlow and McDowell[15] in using a Hartree-Fock momentum distribution find far greater reduction (35%) in the maximum value of the calculated cross section than was observed in the present work using a screened hydrogenic distribution with the same approximate mean kinetic energy of the bound electrons (39.3 vs 39.49 eV, the latter being the expectation value from a Hartree-Fock distribution).

B. Ionization Cross Sections of Medium- and High-Z Atoms

Theories based upon models strictly applicable to hydrogenlike atoms, when compared in detail with real atomic systems, often fail because of dissimilarities between the simple theoretical model and the *complex* atom. In cases in which highly charged projectiles interact with an atomic system, apparent failure in the predictions of the *general* theory may be attributable to failure on the part of the idealized model to describe the highly disrupted atom. Several corrections are given here which may aid in such cases, in the interpretation of anomalous experimental results.

(a) *Increased binding.* Effects giving rise to an increase in the binding of an electron will modify the measured cross section, in general, causing significant reductions at low incident-particle velocities, i.e., for $(mE_1/M_1U)^{1/2} \ll 1$. To a good approximation, the modified cross section for an electron with a ground-state binding energy of U and suffering an increase ΔU, is found from Table I by replacing $v_1^2/\bar{v}^2$ in the first column by

$$(v_1^2/\bar{v}^2)[U/(U+\Delta U)] \tag{6.4}$$

and dividing the result found in the adjacent columns by $(U+\Delta U)^2$. Owing to the steepness of descent at low $v_1^2/\bar{v}^2$ of the excitation functions (columns 2–4), a 5% increase in binding of a $1s$ shell electron at $v_1^2/\bar{v}^2 = 0.0045$ yields an approximate corrected cross section of 0.75 times the uncorrected cross section.

In light of the above, it is of interest to consider an atom under two different conditions. The first state is one in which the neutral atom is ionized in the $1s$ shell with the ejection of exactly one electron. In this case the minimum energy transfer (upon which the cross section is so very sensitive) is given by

$$E_{\min} = U_{1s} = E_{1s^{-1}} - E_{gs}. \tag{6.5}$$

Here E_{1s} is less negative than E_{gs} (the total energy of the ground-state configuration) by exactly the binding of the $1s$ electron. The second condition to consider is one in which a second electron (e.g., $2p$) is ejected during the same particle-atom encounter. In this case the minimum energy transfer is

$$E_{\min} = E_{1s^{-1},2p^{-1}} - E_{gs} > U_{1s} + U_{2p}, \tag{6.6}$$

where U_{2p} is the binding energy for a $2p$ electron in the ground-state configuration [see Eq. (6.5)]. The latter condition in Eq. (6.6) is due to a decrease in the mutual electronic repulsion relative to the ground-state configuration. Using the results of a Hartree-Fock-Slater calculation,[41] we find using iron as an example,

$$\begin{aligned}\Delta E &= (E_{1s^{-1},2p^{-1}} - E_{gs}) - (U_{1s} + U_{2p}) \\ &= 7875.4 - (7066 + 720.2) \\ &= 89.2\ \text{eV}.\end{aligned}$$

Consequently, an increased binding energy of 89 eV must be shared between the two ejected electrons. With the simplifying assumption that this increase is shared evenly, the $1s$ ionization potential in iron is found to increase by 0.6%. Under these assumptions, the corrected cross section at $v_1^2/\bar{v}^2 = 0.0045$ is $\simeq 0.975\,\sigma(v_1^2/\bar{v}^2)$. As has been shown in a number of K x-ray and K Auger-electron measurements[42–45] the probability of removing a considerable number of electrons in a single encounter, even using low-Z projectiles (protons, α's) is quite high. Hence a decrease in the measured cross sections (with respect to the uncorrected) should be evidenced, particularly for low-velocity projectile interactions, with target electrons of moderately low-Z atoms. In Sec. VIC, the problem of estimating the magnitude of multi-

ple ionization shall be considered in more detail.

(b) *Multiple-ionization effects.* As shown in Sec. VI A, the simultaneous removal of both electrons in helium may lead to significant differences between measured ionization cross sections, σ^{gross}, and calculated cross sections, σ^{calc}. In the present section, Eq. (6.1) is generalized to also include cases in which a shell contains an arbitrary number of electrons, N. The ratio of the gross cross section σ^{gross} to the calculated cross section σ^{calc} is then shown to be given by

$$\sigma^{\text{gross}}/\sigma^{\text{calc}} \simeq 1+(N-1)\overline{P}/2$$

provided that, per ionizing event, the average probability of ionization per electron, $\overline{P}$, is substantially less than unity. The probability $\overline{P}$, with some difficulty, can be calculated rigorously from Eq. (6.1), but in lieu of this more detailed treatment a semiempirical estimate is made here which can be useful in estimating the influence of multiple ionization in certain experimental cross-section measurements.

With the assumption that an experimental measurement is unable to discriminate between single- and multiple-ionizing events in a shell containing N electrons, Eq. (6.3) can be more generally written as

$$\sigma^{\text{gross}} = \sum_{i=1}^{N} i({}_i\sigma),$$

where ${}_i\sigma$ is the cross section for ejection of exactly i electrons from the shell. The calculated cross section, on the other hand, is given by

$$\sigma^{\text{calc}} = \sum_{i=1}^{N} {}_i\sigma.$$

Consequently,

$$\frac{\sigma^{\text{gross}}}{\sigma^{\text{calc}}} = 1+\sum_{i=1}^{N}(i-1)\,{}_i\sigma/\sigma^{\text{calc}}, \tag{6.7}$$

where σ^{calc} is given by Eq. (5.1). The partial cross sections ${}_i\sigma$ in Eq. (6.7) are given by

$${}_i\sigma = 2\pi\int_0^{\infty}\frac{N!}{(N-i)!\,i!}\,\hat{P}^i(b)[1-\hat{P}(b)]^{N-i}\,b\,db \tag{6.8}$$

under the condition that the removal of each electron does not influence (increase the binding of) the other electrons [see Eq. (6.3)]. It follows then that

$$\frac{\sigma^{\text{gross}}}{\sigma^{\text{calc}}} = 1+\sum_i \frac{(i-1)(N-1)!}{(N-i)!\,i!}\langle \hat{P}^{i-1}(b)[1-\hat{P}(b)]^{N-i}\rangle, \tag{6.9a}$$

where

$$\langle \hat{P}^{i-1}(b)[1-\hat{P}(b)]^{N-i}\rangle = \frac{(N-i)!\,i!}{(N-1)!}\,\frac{{}_i\sigma}{\sigma^{\text{calc}}}. \tag{6.9b}$$

If the average probability of ionization per electron, $\overline{P}$, is much less than unity, then Eq. (6.9a) is found to reduce to

$$\frac{\sigma^{\text{gross}}}{\sigma^{\text{calc}}} \approx 1+(N-1)\langle\hat{P}(b)\rangle/2 \equiv 1+(N-1)\overline{P}/2. \tag{6.10}$$

The probability $\overline{P}$ has been semiempirically derived in the present work by assuming that the incident particle on the average interacts only at the "adiabatic" radius.[46] The constant (7×10^{-5}) was estimated from the exact calculations for $\overline{P}$ for the $1s$, $2s$, and $2p$ shells of several elements. The probability $\overline{P}$ was found to be

$$\overline{P} \simeq \frac{7\times10^{-5}Z^2q^2}{U^2(\text{keV})^2n^3(l+\frac{1}{2})}\ \text{keV}^2\left(\frac{\bar{v}}{v_1}\right)\frac{\hat{\sigma}(v_1^2/\bar{v}^2)}{\hat{\sigma}(v_1^2/\bar{v}^2=1)}, \tag{6.11}$$

with Z and q the charges of the target element and projectile, respectively. U is the binding energy in keV, n and l are the principle and angular-momentum quantum numbers, and $\bar{v}/v_1 = (MU/mE)^{1/2}$. The quantities $\hat{\sigma}(v_1^2/\bar{v}^2)$ may be taken from Table I.

(c) *Decrease of the incident-particle kinetic energy in the vicinity of the nucleus.* As had been discussed previously[4,10,11] during close encounters with the nucleus, the positively charged projectile suffers a decrease in kinetic energy, counteracting its increase of potential energy in the repulsive Coulomb field of the nucleus. This decrease in kinetic energy will at low incident-particle velocities result in a significant decrease in the ionization cross section, which can be accounted for exactly only in impact-parameter theories such as the present. For theories in which this correction cannot be applied continuously as a function of the incident particle's distance from the nucleus, one can nevertheless correct for this effect provided one knows the average distance from the nucleus at which ionizing events occur. This average distance is defined to be the adiabatic radius, r_{ad}, and is given by[47]

$$r_{\text{ad}} = \frac{\hbar w_1}{\Delta E} = \frac{2v_1}{\bar{v}}\,\frac{a_0 n}{Z} = \frac{2v_1}{\bar{v}}\,a_Z,$$

where $v_1/\bar{v} = (mE_1/MU)^{1/2}$, $a_0 = 5.29\times10^{-9}$ cm, n is the principle quantum number, and Z the nuclear charge.

The cross section corrected for this effect can be found using Table I by replacement of $v_1^2/\bar{v}^2$ by

$$v_1^2/\bar{v}^2 - nm\bar{v}q/Mv_1, \tag{6.12}$$

where n is the principle quantum number, q the projectile charge, and m/M the ratio of electron to projectile masses. Equation (6.12) has been derived by assuming that the incident particle interacts at the adiabatic radius with a consequent

loss of kinetic energy, prior to ionization, of qZe^2/r_{ad}.

(d) *Appropriate momentum distribution.* As discussed in Sec. III, replacement of Z_{eff}/n by $(U/\mathcal{R})^{1/2}$ where $\mathcal{R}$ is the Rydberg energy in the wave function describing the bound electron leads to a convenient set of scaling laws discussed in detail elsewhere[4,11,12] and given in Eq. (3.4).

A more appropriate Z_{eff} is probably found by use of semiempirical screening rules, e.g., Slater rules.[48] The ionization cross section has been shown to be relatively insensitive to substantial changes in the momentum distribution of the bound electron (see, for example, Fig. 2, p. 339, Ref. 4 and Figs. 1–3 of this paper). As pointed out in Sec. VI A, one of the effects of an increase in the mean kinetic energy of the bound electrons is to shift the maximum in the cross section to higher incident-particle energies. Therefore, in cases where $(U_K/\mathcal{R})/(Z-0.3)^2$ or $(n^2U_L/\mathcal{R})/(Z-4.15)^2$ is significantly less than unity, one might expect the maximum cross section to occur at somewhat higher projectile energies than $E_1 = M_1U/m$.

(e) *Relativistic effects.* For medium- and high-Z atoms, the innermost electrons, during close encounters with the nucleus, can reach extreme relativistic velocities (e.g., in Au an electron at $0.1a_0/79$ attains an average kinetic energy of approximately 1.3 MeV). In a more exact BEA theory, one should use relativistic expressions for the wave functions of the electron in order to generate the proper momentum distribution. An approximate correction can be made in lieu of a more detailed treatment by assuming the kinetic energy of the bound electron to be given correctly by the nonrelativistic equations $E_2 = \frac{1}{2}m_0v_2^2$. Relativistic equations can then be used to determine the relativistic mass and velocity. In the present case we have taken v_2 from Eq. (4.2) and found the relativistic velocity V_{rel} and mass m from

$$V_{rel} = [R/(1+R)]^{1/2}(c)$$

and

$$m = m_0/(1-\beta^2)^{1/2},$$

where $R = (E_2/m_0c^2)^2 + 2(E_2/m_0c^2)$ and $\beta = V_{rel}/c$. In these equations, c is the velocity of light and m_0 the rest mass of an electron.

Table II gives the ratio of corrected ($1s$) cross sections to the uncorrected ($1s$) cross sections, as found in this manner, each as a function of $E_1m/UM = v_1^2/\bar{v}^2$. The magnitude of the correction increases at low incident-particle velocities since in this case ionizing events must involve electrons in the high-velocity portion of the velocity distribution in order to conserve momentum during the interaction[4] (see Sec. VI B c).

TABLE II. Relativistic corrections.

	$\sigma^{rel}/\sigma^{nonrel}$			
$(v_1/\bar{v})^2$	$Z=29$	$Z=47$	$Z=73$	$Z=92$
1.2×10^{-2}	1.34	2.44	5.85	10.2
1.81×10^{-2}	1.22	1.736	3.21	5.17
2.7×10^{-2}	1.146	1.48	2.38	3.53
4.0×10^{-2}	1.096	1.31	1.87	2.56
7.3×10^{-2}	1.05	1.16	1.44	1.755
1.6×10^{-1}	1.02	1.06	1.17	1.28
3.6×10^{-1}	1.014	1.04	1.09	1.15
9.9×10^{-1}	1.01	1.02	1.05	1.07
4.0×10^{0}	0.99	0.96	0.89	0.81
2.4×10^{1}	0.97	0.91	0.82	0.75

In a recent paper it has been observed in high-Z atoms that measured K-shell ionization cross sections at low incident-particle velocities ($v_1/\bar{v}\,\frac{n}{k} < 0.7$) rise consistently higher than the BEA predictions. With increasing target Z the experimental data deviates further above the BEA curve, being as much as a factor of 2 above for gold in the velocity range $v_1/\bar{v} \simeq 0.4$. A simple "semi-relativistic" correction to the experimental data is used in Ref. 49 which clusters the data around a single experimental curve which falls below the BEA curve by approximately 15% in the velocity range surrounding $v_1/\bar{v} = 0.4$. Corrections to their experimental data, using the values from Table II, appear to cluster the data more closely about the BEA curve. A detailed comparison of these relativistic effects shall be the subject of a future paper.

C. Multiple Ionization

A distinct advantage which the configuration-space BEA has over its momentum-space counterpart is that the former, when expressed in cylindrical coordinates, gives the impact-parameter representation. In this section we apply the impact-parameter representation of the BEA to the problem of simultaneous Coulomb ejection of bound electrons from different shells.

The first part, Sec. VI C a, uses as an example the simultaneous ejection of electrons from the $n=1$ and $n=2$ shells in order to develop the general formulation of the problem.

In Sec. VI C b we compare the present theoretical predictions with the predictions from a SCA calculation[50] as well as with recent experimental results[51] for the probability of simultaneous $K+L$ shell ionization. Also, the problem studied earlier[51] of the influence of L-shell vacancy shifts upon measured $K+L$-shell multiple-ionization probabilities is reconsidered.

In Sec. VI C c, approximate formulas enabling one to estimate the magnitude of multiple ionization are derived from preceding formulas and the validity of the approximations considered.

(a) *General formulation.* In order to develop the rigorous formulas it is convenient to concentrate upon a specific example. Quite arbitrarily, the cross sections and probabilities related to ejection of one or more L-shell ($2s$) electrons during events which give rise to ionization in the K shell ($1s$) shall be given.

Noting that the total K-shell cross section may be expressed as $\sigma_K = \sum_{i=0}^{N_{L_1}} {}_i\sigma_{KL}$, the partial K-shell cross section ${}_i\sigma_{KL}$ for ejecting exactly i L_1 electrons during a collision ionizing the K shell is then given by[50]

$$ {}_i\sigma_{KL} = 2\pi \int_0^\infty bP_K(b)[1-\hat{P}_{L_1}(b)]^{N_{L_1}-i}\hat{P}^i_{L_1}(b)C^{N_{L_1}}_i\,db, \tag{6.13a} $$

where the $\hat{P}(b)$'s are probabilities for ionization *per* electron, the binomial coefficients $C^{N_{L_1}}_i$ are defined as $N_{L_1}!/(N_{L_1}-i)!i!$, and $N_{L_1}=2$ in the case of the L_1 subshell.

The probability ${}_iP_{KL_1}$ of ejecting exactly i electrons from the L_1 subshell per K-shell ionization is thus found by dividing Eq. (6.13a) by the total K-shell cross section σ_K. Consequently,

$$ {}_iP_{KL_1} = \langle [1-\hat{P}_{L_1}(b)]^{N_{L_1}-i}[\hat{P}^i_{L_1}(b)]\rangle \tag{6.13b} $$

where the quantity within $\langle\,\rangle$ has been explicitly averaged over the distribution given in Eq. (5.1).

Often of further interest is the cross section σ_{KL_1} and probability P_{KL_1} of ejecting one or more external (L_1) electrons. This only requires an appropriate summation to be carried out over formulas (6.13a) and (6.13b), respectively. Hence

$$ \sigma_{KL_1} = \sum_{i=1}^{N_{L_1}} \int_0^\infty 2\pi b P_K(b)[1-\hat{P}_{L_1}(b)]^{N_{L_1}-i}\hat{P}^i_{L_1}(b)C^{N_{L_1}}_i\,db \tag{6.14a} $$

and

$$ P_{KL_1} = \sigma_{KL_1}/\sigma_K\,. \tag{6.14b} $$

Taking advantage of the properties of the binomial expansion, the last equation can be reexpressed as[50]

$$ P_{KL_1} = \frac{\int_0^\infty 2\pi b P_K(b)\{1-[1-\hat{P}_{L_1}(b)]^{N_{L_1}}\}\,db}{\sigma_K} \tag{6.15} $$

or more simply

$$ P_{KL_1} = \langle 1-[1-\hat{P}_{L_1}(b)]^{N_{L_1}}\rangle. \tag{6.16} $$

The product $N_{L_1}\langle\hat{P}_{L_1}(b)\rangle$ is the *average number of* L_1 *electrons* ejected per ionizing event and as the probability of ejecting more than a single L_1 electron per ionizing event becomes small, i.e., $N_{L_1}\langle\hat{P}_{L_1}(b)\rangle \ll 1$, we find

$$ P_{KL_1} \approx N_{L_1}\langle\hat{P}_{L_1}(b)\rangle \quad \text{for } N_{L_1}\langle\hat{P}_{L_1}(b)\rangle \ll 1. \tag{6.17} $$

Expressions identical in form are found for the $2p$ shell (or any shell) by using the correct $\hat{P}(b)$ for the subshell in question and summing over the number of electrons in the shell considered.

One final expression necessary to compute the probability, P^{tot}_{KL}, of ejection of one or more electrons from a total shell, e.g., the L shell, is the following

$$ P_{KL} = 1-(1-P_{KL_1})(1-P_{KL_{23}}) \tag{6.18a} $$

$$ \approx P_{KL_1}+P_{KL_{23}} \quad \text{provided } P_{KL_1}P_{KL_{23}} \ll 1 $$

$$ \approx N_{L_1}\langle\hat{P}_{L_1}(b)\rangle + N_{L_{23}}\langle\hat{P}_{L_{23}}(b)\rangle, \tag{6.18b} $$

where $\hat{P}_{L_{23}}(b)$ is the probability of ionization per $2p$ electron for a projectile with impact parameter b.

(b) *Comparison with experiment and with the predictions of the* SCA. Using the preceding expressions, theoretical values for the probability of one or more L-shell electrons being ejected per K-shell ionization were found. These are compared with the recent experimental measurements of Li *et al.*[51] in Fig. 12. In general, the shape of the theoretical curve is borne out in the

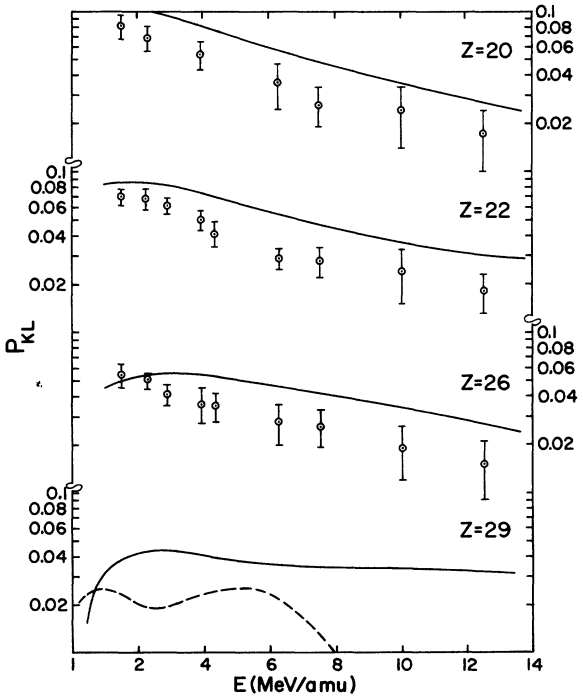

FIG. 12. Comparison of present theoretical values of P_{KL} with the experimental values at $Z=20$, 22, 26 from Ref. 51 and with the theoretical values at $Z=29$ from Ref. 49.

experimental findings with experimental results falling systematically below the present theoretical predictions. In Fig. 12, a comparison at $Z=29$ of the present calculated values of P_{KL} is also made with recent values calculated[50] using the SCA. The poor agreement probably reflects the discrepancies which exist between the calculated L-shell cross sections (see Figs. 2 and 3).

In Ref. 51, the probability of L-shell vacancy shifts was considered, i.e., the experimental results measured the probability of an L vacancy being present when a K x ray was emitted. Consequently they have shown that the values of P_{KL}^{corr} corrected for this effect are related to the uncorrected values P_{KL}^{unc} by

$$P_{KL}^{\text{corr}} = [(\Gamma_K + \Gamma_{L_3})/\Gamma_K]\, P_{KL}^{\text{unc}}, \tag{6.19}$$

where Γ_K and Γ_{L_3} are the average level widths[52] for the K and L_3 shells, respectively.[53] A derivation of Eq. (6.19) is found in Ref. 51 along with a discussion of its expected accuracy.

In the present work, the correction factor $C_f = (\Gamma_K + \Gamma_{L_3})/\Gamma_K$ has been deduced from our theoretical P_{KL} and from P_{KL}^{unc} from Ref. 51, and is shown in Fig. 13 for $_{20}$Ca, $_{22}$Ti and $_{26}$Fe. For each element, values of C_f were derived at the experimental energies shown in Fig. 12. The data points, in Fig. 13, are the averages of these C_f for each element and the error bars represent the maximum variation of C_f from the mean value. Also shown are the values of C_f, taken from Ref. 51, and computed from the values of Γ_{L_3} as calculated by Chen *et al.*[54] and by McGuire.[55] These two calculations differ radically and neither fit our derived values of C_f. The total K width (Γ_K in C_f) was computed in Ref. 51 from $\Gamma_K = \Gamma_K^R/\omega_K$, where Γ_K^R is the total radiative width of the K level[56] and ω_K the K-shell fluorescence yield.[53] The comparison made in Fig. 13 presupposes that the total level widths Γ_K and Γ_{L_3} in Eq. (6.19), representing states with an L plus a K vacancy, do not differ significantly from Γ_K and Γ_{L_3} representing states containing but a single vacancy in the K and L shells, respectively. Also in the computation[51] of the correction factor C_f from Eq. (6.19), associated uncertainties in the determination of Γ_K^R and ω_K were not considered.

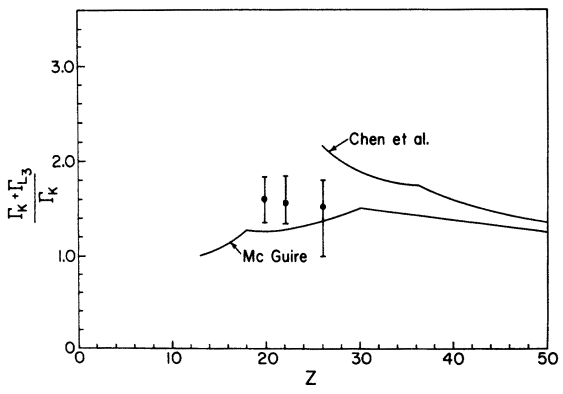

FIG. 13. Correction $(\Gamma_K + \Gamma_L)/\Gamma_K$. The curves labeled Chen *et al.* and McGuire have been computed using theoretical values of Γ_L from Refs. 54 and 55, respectively. The total width of the K state, Γ_K, in both cases is the same (see text). Experimental values found from combining present theory with experimental results from Ref. 51.

(c) *Derivation of approximate formulas.* Analytical formulas for the probability of multiple ionization can be derived from the equations in Sec. VI C a provided certain approximations are made. These formulas do not, in general, agree well with the rigorous results because of the severity of certain of the necessary approximations. They may be useful, nevertheless, in estimating the magnitude of multiple ionization and its consequent effect in experimental measurements. If the condition given in Eq. (6.18a) holds for the L_1 and L_{23} subshells, we may approximate the probability of ejecting one or more L shell electrons from Eq. (6.18b), i.e.,

$$P_{KL} \approx P_{KL_1} + P_{KL_{23}} \approx 2\langle \hat{P}_{L_1}(b)\rangle + 6\langle \hat{P}_{L_{23}}(b)\rangle. \tag{6.20}$$

Assuming further that $P_{L_1}(b) \simeq P_{L_1}(0)$ and $P_{L_{23}}(b) \simeq P_{L_{23}}(0)$ [see Eq. (6.15)], i.e., the probability of L-shell ionization over the "mean" K-shell dimensions is approximately the same as the probability at $b=0$, then $P_{KL}^{\text{tot}} = 2\langle \hat{P}_{L_1}(0)\rangle + 6\langle \hat{P}_{L_{23}}(0)\rangle$, but from Eq. (5.3),

$$\hat{P}_{L_1}(b) = \int_0^\infty \hat{\sigma}(r)\rho_{L_1}(r)\,dz = 2\int_0^\infty \frac{\hat{\sigma}(r)\bar{\rho}_{L_1}(r)4\pi z^2 \rho_{L_1}(z)\,dz}{4\pi z^2 \rho_{L_1}(z)}, \tag{6.21}$$

with $r = (b^2 + z^2)^{1/2}$. Then

$$P_{L_1}(0) = 2\left\langle \frac{\hat{\sigma}_{L_1}(z)}{4\pi z^2}\right\rangle \approx \frac{\langle \hat{\sigma}_{L_1}\rangle}{2\pi}\langle 1/z^2\rangle_{L_1}. \tag{6.22}$$

Also,

$$P_{L_{23}}(0) \approx \frac{\langle \hat{\sigma}_{L_{23}}\rangle}{2\pi}\langle 1/z^2\rangle_{L_{23}}, \tag{6.23}$$

where $\langle \hat{\sigma}\rangle$ in both cases is the cross section per *electron* (Table I). The average value $\langle 1/z^2\rangle$ for screened hydrogenlike atoms is given by[18]

$$\langle 1/z^2\rangle = \frac{Z_{\text{eff}}^2}{n^3(l+\frac{1}{2})}\,\frac{1}{a_0^2}. \tag{6.24}$$

Consequently, combining expressions (6.22) and (6.23) and using Eq. (6.24):

$$P_{KL} \simeq \frac{\bar{\sigma}_L Z_{\text{eff}}^2}{2\pi a_0^2} ;$$

$$\bar{\sigma} = \tfrac{1}{2}(\hat{\sigma}_{L_1} + \hat{\sigma}_{L_{23}}), \tag{6.25}$$

where $\hat{\sigma}_{L_1}$ and $\hat{\sigma}_{L_{23}}$ are the cross sections per electron for the L_1 and L_{23} subshells, respectively, as found from Table I. Therefore,

$$P_{KL} = 6\times 10^{-9}\,\bar{\sigma}_L(b) Z_{\text{eff}} \tag{6.26}$$

for incident protons. For projectiles of charge q within the limits of the above approximations, we can assume $P_{KL}(q) = q^2 P_{KL}(q=1)$. In general, Eq. (6.26) gives only a very crude estimate of the probability of multiple ionization. What appears to be the most serious of the above approximations leading to Eq. (6.26), is made in Eq. (6.22) and (6.23), namely, $\langle F(x)/G(x)\rangle = \langle F(x)\rangle\langle 1/G(x)\rangle$. Because of the strong dependence of the ionization cross section upon the velocity of the bound electron and therefore upon the distance z from electron to nucleus, the approximation made in these equations might be expected to lead to considerable error.

In the velocity region, $v_1 \sim v_L$, a partial account for the z dependence of σ_L was made in the present work, and a somewhat *more accurate estimate* of P_{KL} was empirically found to be a *factor of* 3 less than that predicted by Eq. (6.26). Finally one must recall that Eq. (6.26) has been derived with the assumption that the probability of ionization per electron is small, or more precisely $N\hat{P} \ll 1$. If this condition is not met, e.g., if $P_{KL} > 1$, the value more closely corresponds to the average number of L shell electrons ejected during a collision and the probability of one or more electrons being ejected will be better described using the constrained BEA definition, i.e., by replacing P_{KL} by $1 - e^{-P_{KL}}$.

VII. SUMMARY AND CONCLUSIONS

A configuration-space formulation of the BEA has been carried out following a transformation which relates the velocity of an electron to its distance from the nucleus. This new representation of the BEA appears more successful in some areas, e.g., ionization of He by protons, when compared with the conventional momentum-space version of the BEA. The new representation also allows us to calculate multiple-ionization probabilities and further provides corrections which facilitate direct comparisons of the predictions of the BEA with multielectron-atom experimental results.

The calculated ionization probabilities from this new model of course depend directly upon the form of the transformation $v(r)$. At an early stage of this work, classical rules for $v(r)$ based upon conservation of energy were seen to lead to very nonphysical pictures of the atom, e.g., imaginary velocities, or "holes" in the central regions of the atom for the $2p$ states. The present $v(r)$ transformation does not in this way create false images of the atom and does appear to predict reasonably well the ionization probability as a function of impact parameter (Fig. 6). The $v(r)$ prescription is idealized in the sense of assigning exactly one velocity for each r. At low incident-particle velocities, this will lead to overestimations of the probability of ionization during close encounters with the nucleus and underestimate the probability for more distant encounters. The assignment of a distribution of velocities at each point, based perhaps upon the Heisenberg uncertainty principle, would be of physical interest but computational time might well become prohibitive except in a few simple problems.

In the case of ionization of hydrogen by protons, the model and the real system are very nearly identical (save for the presence of the nucleus) so the inherent approximations of the BEA are rigorously tested. The present results seem to favor the lower of two sets of experimental data, whereas the unrestricted BEA is in good agreement with the higher of the two sets of experimental data. At low energies, the present calculated cross sections for hydrogen tend to lie above the experimental results. Vriens has pointed out that because of an overlap of energy regions, the calculated BEA ionization cross section actually includes a part of the electron exchange cross section. For incident-proton velocities less than the mean orbital velocity of the electron, this suggests that the BEA *should* overestimate the true ionization cross section. The neglect of the presence of the third body (another proton) will also lead to error. Classical three-body calculations[57] do appear to be in far better agreement with the low-energy experimental data than are the two-body calculations.

In the case of He, charge exchange and the presence of the nucleus, both neglected in the present theory, will also influence the ionization cross sections. In addition, the effects of electron correlation in He are neglected and, consequently, the multiple-ionization cross sections given here are done so with the assumption that correlation effects are negligible. To correctly account for these correlation effects would require a much more detailed treatment than is presented here.

The energy-exchange FPC as used here was derived on the basis of an isotropic distribution of field-particle velocity vectors.[5,6] In the special case of atoms prealigned with respect to the incident beam, lack of isotropy in the electron mo-

mentum distribution has been shown to lead to differences in calculated cross sections.[58] We have assumed throughout that the target atoms have no preferred alignment with respect to the incident beam, hence justifying the use of the FPC as derived in Refs. 5 and 6.

A point which the present author has become aware of through comparisons of the predictions of this theory and others is that owing often to "poor" selection of fluorescence yields (the conversion factor from x-ray yields to cross sections) or use of inappropriate binding energies, apparent experimental-theoretical corroboration has been achieved in some cases. In the present paper, the author has used only experimental binding energies. Far better agreement with the experimental results in the case of the proton-helium ionization problem could be achieved by using a suitably selected semiempirical binding energy but no sound basis for such a selection could be found.

Finally, in the case of multiple ionization, we have neglected those interactions which involve the ejection of a bound electron which during its departure from the atom ejects a second electron. Cascading effects such as this can be shown to become important only at relatively high incident-particle velocities (see, for example, Ref. 4). Also very weakly bound electrons will be subject to ejection via the shakeoff process, i.e., an inability on the part of such electrons to adiabatically adjust to the ionic potential arising when a neutral atom is ionized in one of its inner shells. This important complementary multiple-ionization process has been recently reviewed by Krause.[59]

Note added in proof. More extensive tabulations of Table I ($3s$, $3p$, and $3d$ subshells) and of Table II (even $Z > 28$) are available from the author upon request.

ACKNOWLEDGMENTS

The pioneering work of Dr. Michal Gryziński was essential to the development of the present theory. The earlier experimental work of Dr. R. L. Watson and numerous discussions with him of the ionization problem were very useful. Dr. J. F. Reading generously aided the author in the conceptualization of several of the more fundamental ideas of collision theory. The advice of Dr. M. Jain with regard to numerical techniques and the properties of the Fourier transformation was most useful. A close association with Dr. J. H. McGuire during the preliminary stages of this work was of great benefit. Dr. M. Jain, Dr. J. F. Reading, Dr. R. L. Watson, and R. W. Howard provided critical reviews of the manuscript and offered many useful suggestions for which the author is much indebted. The advice of Dr. Dwight Saylor relating to refinements of ideas in Sec. V is gratefully acknowledged. Mrs. J. S. Hansen devoted many weeks to manuscript preparation for which the author extends his humblest thanks.

---

*Work supported by the U. S. Atomic Energy Commission, the Robert A. Welch Foundation, and the U. S. Air Force Office of Scientific Research (No.732484).

[1]J. J. Thomson, Philos. Mag. **23**, 449 (1912).
[2]Michal Gryziński, Phys. Rev. **107**, 1471 (1957).
[3]Michal Gryziński, Phys. Rev. **115**, 374 (1958).
[4]Michal Gryziński, Phys. Rev. **138**, A305 (1964).
[5]E. Gerjuoy, Phys. Rev. **148**, 54 (1966).
[6]L. Vriens, Proc. Phys. Soc. Lond. **90**, 935 (1967).
[7]M. R. C. McDowell, Proc. Phys. Soc. Lond. **89**, 23 (1966).
[8]J. D. Garcia, E. Gerjuoy, and J. E. Welker, Phys. Rev. **165**, 66 (1967).
[9]L. Vriens, Physica (Utr.) **49**, 602 (1970); D. R. Bates and W. R. McDonough, J. Phys. B **3**, L83 (1970).
[10]J. D. Garcia, Phys. Rev. A **1**, 280 (1970).
[11]J. D. Garcia, Phys. Rev. A **1**, 1402 (1970).
[12]E. W. McDaniel and M. R. C. McDowell, *Case Studies in Atomic Collision Physics I* (North-Holland, Amsterdam, 1969).
[13]M. R. C. McDowell and J. P. Coleman, *Introduction to the Theory of Ion-Atom Collisions* (North-Holland, Amsterdam, 1970).
[14]J. B. Hasted, *Physics of Atomic Collisions* (Butterworths, Washington, 1964).
[15]G. W. Catlow and M. R. C. McDowell, Proc. Phys. Soc. Lond. **92**, 875 (1967).
[16]L. Vriens and T. F. M. Bonson, J. Phys. B **1**, 1123 (1968).
[17]Here and throughout the remainder of the present paper, in order to avoid possible ambiguities, we shall distinguish between the cross section per electron $\hat{\sigma}$ and the measured cross section σ which follows from summing over the electrons within the shell.
[18]H. A. Bethe and E. E. Salpeter, *Quantum Mechanics of One- and Two-Electron Atoms* (Academic, New York, 1957).
[19]I. N. Sneddon, *Fourier Transforms* (McGraw-Hill, New York, 1961).
[20]A. N. Tripathi, K. C. Mathur, and S. K. Joshi, J. Phys. B **2**, 878 (1969).
[21]L. Vriens, in *Proceedings of the Sixth International Conference on the Physics of Electronic and Atomic Collisions: Abstracts* (MIT Press, Cambridge, Mass., 1969).
[22]J. M. Hansteen and O. P. Mosebekk, Technical Report No. 39, University of Bergen, Norway, 1971 (unpublished).
[23]E. Merzbacher, in *Proceedings of the International Conference on Inner-Shell Ionization Phenomena*, Atlanta, Ga. (U.S.AEC Technical Information Center, Oak Ridge, Tenn., 1973).
[24]V. Fock, Z. Phys. **98**, 145 (1935).
[25]Previous comparisons of the results of the SCA and BEA for the $1s$ state have shown them to be in excellent agreement, see Ref. 26.
[26]J. D. Garcia, R. J. Fortner, and T. M. Kavanaugh, Rev. Mod. Phys. **45**, 111 (1973).
[27]A. Messiah, *Quantum Mechanics* (North-Holland, Amsterdam,

1962).
[28]In the present paper, except where noted, the charge distribution $\rho_{n,l}(r)$ was obtained through the use of $Z_{\text{eff}} = n\,[U/Ry]^{1/2}$ in order to take advantage of the scaling law in Eq. (3.4).
[29]Per electron probabilities shall be designated throughout as $\hat{P}$.
[30]E. Laegsgaard, J. V. Anderson, and L. C. Feldman, Phys. Rev. Lett. **29**, 1206 (1972).
[31]Unitarity violations can also occur for transitions between close levels in the Born approximation. Seaton has considered several aspects of this problem in Ref. 32.
[32]M. J. Seaton, Proc. Phys. Soc. Lond. **77**, 184 (1961).
[33]W. L. Fite, R. F. Stebbings, D. G. Hummer, and R. T. Brackmann, Phys. Rev. **119**, 663 (1960).
[34]H. B. Gilbody and J. V. Ireland, Proc. R. Soc. A 277, 137 (1963).
[35]Mitio Inokuti, Rev. Mod. Phys. **43**, 297 (1971).
[36]N. V. Federenko, V. V. Afrosimov, R. N. Il'in, and E. S. Solov'ev, *Proceedings of the Fourth International Conference of Ionization Phenomena in Gases* (North-Holland, Amsterdam, 1960), Vol. IA, p. 47.
[37]J. W. Hooper, D. S. Harmer, O. W. Martin, and E. W. McDaniel, Phys. Rev. **125**, 2000 (1962).
[38]F. J. DeHeer, J. Schutten, and H. Moustafa, Physica (Utr.) **32**, 1766 (1966).
[39]J. T. Park and F. D. Schowengerdt, Phys. Rev. **185**, 152 (1969).
[40]G. Peach, Proc. Phys. Soc. Lond. **85**, 709 (1965).
[41]F. Herman and S. Skillman, *Atomic Structure Calculations* (Prentice-Hall, Englewood Cliffs, N. J., 1963).
[42]D. Burch, P. Richard, and R. S. Blake, Phys. Rev. Lett. **26**, 1355 (1971).
[43]J. S. Hansen, T. K. Li, and R. L. Watson, in Ref. 23.
[44]A. R. Knudson, D. J. Nagle, P. G. Burkhalter, and K. L. Dunning, Phys. Rev. Lett. **26**, 1149 (1971).
[45]R. L. Watson and L. H. Toburen, Phys. Rev. (to be published).
[46]The adiabatic radius is defined in the first equation of the following section [Sec. VI B c].
[47]J. Bang and J. M. Hasteen, K. Dan. Vidensk. Selsk. Mat.-Fys. Medd. 31 (1959).
[48]H. Eyring, J. Walter, and G. E. Kimball, *Quantum Chemistry* (Wiley, New York, 1967).
[49]T. L. Hardt and R. L. Watson, Phys. Rev. A (to be published).
[50]J. M. Hansteen and O. P. Mosebekk, Phys. Rev. Lett. **29**, 1361 (1972).
[51]T. K. Li, R. L. Watson, J. S. Hansen, Phys. Rev. A (to be published).
[52]Here and in Ref. 51, that portion of each subshell level width associated with Coster-Kronig transfers, i.e., intra-shell transfers, has been excluded in the determination of Γ_L.
[53]W. Bambynek, B. Crasemann, R. W. Fink, H-U. Freund, H. Mark, C. D. Swift, R. E. Price, and P. V. Rao, Rev. Mod. Phys. **44**, 716 (1972).
[54]M. H. Chen, B. Crasemann, and V. O. Kostroun, Phys. Rev. A **4**, 1 (1971).
[55]E. J. McGuire, Phys. Rev. **185**, 1 (1969).
[56]J. H. Scofield, Phys. Rev. **179**, 9 (1969).
[57]R. Abrines and I. C. Percival, Proc. Phys. Soc. Lond. **88**, 873 (1966).
[58]D. Banks, L. Vriens, and T. F. M. Bonson, J. Phys. B **2**, 976 (1969).
[59]M. O. Krause, in Ref. 23.

PHYSICAL REVIEW A VOLUME 8, NUMBER 2 AUGUST 1973

Total Cross Sections for Inelastic Scattering of Charged Particles by Atoms and Molecules. VII. The Neon Atom*

Roberta P. Saxon
Argonne National Laboratory, Argonne, Illinois 60439
(Received 5 January 1973)

The Bethe theory for the calculation of the total inelastic cross section σ_{tot} for the scattering of fast charged particles by atoms and molecules is applied to neon. As part of the analysis, the spectral distribution of the oscillator strength has been determined by critical evaluation of all experimental data and by test of several sum rules. The result is $\sigma_{\text{tot}} = z^2\beta^{-2}\{3.524[\ln(\beta^2/(1-\beta^2)) - \beta^2] + 36.06\} \times 10^{-20}$ cm^2 for a particle of charge ze and speed βc. As an application, the ionization cross section is estimated by subtracting the sum of all the discrete excitation cross sections from σ_{tot} and is compared with experimental values.

I. INTRODUCTION

In recent years renewed interest has been seen in the study of inelastic scattering of charged particles by atoms and molecules. The basic theory for treating fast incident particles, within the Born approximation, was developed by Bethe[1] in the 1930s, but its definitive application to anything other than atomic hydrogen was limited by the lack of reliable wave functions. More modern considerations began with the study of He by Inokuti, Kim, and Platzman,[2] who utilized a powerful sum rule to reduce the calculation of the total inelastic scattering cross section to two separate tasks: first, analysis of optical oscillator-strength data, and second, calculation of certain properties from ground-state wave functions. This work has been followed by careful treatments of other two-elec-